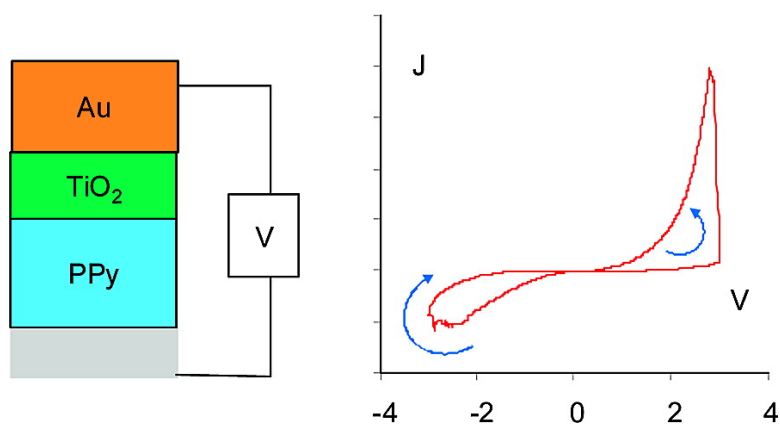


Conducting Polymer Memory Devices Based on Dynamic Doping

Sudip Barman, Fengjun Deng, and Richard L. McCreery

J. Am. Chem. Soc., **2008**, 130 (33), 11073-11081 • DOI: 10.1021/ja802673w • Publication Date (Web): 23 July 2008

Downloaded from <http://pubs.acs.org> on February 8, 2009



More About This Article

Additional resources and features associated with this article are available within the HTML version:

- Supporting Information
- Access to high resolution figures
- Links to articles and content related to this article
- Copyright permission to reproduce figures and/or text from this article

[View the Full Text HTML](#)

Conducting Polymer Memory Devices Based on Dynamic Doping

Sudip Barman, Fengjun Deng, and Richard L. McCreery*

National Institute for Nanotechnology, Department of Chemistry, University of Alberta,
Edmonton, Alberta, Canada T6G 2M9

Received April 11, 2008; E-mail: mcreery@ualberta.ca

Abstract: Molecular electronic junctions consisting of a 20 nm thick layer of polypyrrole (PPy) and 10 nm of TiO₂ between conducting layers of carbon and gold were investigated as potential nonvolatile memory devices. By making the polymer layer much thinner than conventional polymer electronic devices, it is possible to dynamically oxidize and reduce the polypyrrole layer by an applied bias. When the electrode in contact with the PPy is biased positive, oxidation of the PPy occurs to yield a conducting polaron state. The junctions exhibit a large increase in conductance in response to the positive bias, which is reversed by a subsequent negatively biased pulse. Switching between the conducting and nonconducting state can occur for pulses at least as short as 10 μ s, and the conducting state persists after a positive bias pulse for at least 1 week. The read/write/read/erase cycle may be repeated for at least 1700 cycles, although with an error rate of \sim 3% due mainly to an incomplete “erase” step. The speed and retention of the PPy/TiO₂ junctions are far superior to those of the analogous fluorene/TiO₂ devices lacking the polymer, and the conductance changes are absent if SiO₂ is substituted for TiO₂. The observations are consistent with “dynamic doping” of the solid-state polymer layer, with the possible involvement of adventitious mobile ions. Although the speed of the current polymer/TiO₂ junctions is slower than commercial dynamic random access memory, their retention is \sim 5 orders of magnitude longer.

Introduction

Memory devices in widespread use in microelectronics are of two general types: “dynamic”, with short retention times and fast write/read/erase times, and “nonvolatile”, with retention of $>$ 10 years and slower access and write times than dynamic memory. The common forms of these devices are dynamic random access memory (DRAM), with access times in the region of 10 ns and retention $<$ 100 ms, and the hard disk or “flash” memories, with access times of microseconds to milliseconds but retention of several years. Despite many attempts, commercially viable alternatives to these common technologies have not emerged, even though there is a significant range of access times and volatility between the two extremes. Examples relevant to the current report include memory devices based on metal filament formation in solid electrolytes,^{1,2} ion motion in conducting polymers,^{3–6} trapped charge in organic light-emitting diodes,⁷ and molecular memory based on redox activity of

rotaxanes in crossbar circuits.^{8,9} Memory technology based on bias-induced migration of ions in conducting polymers was recently investigated for commercial application by Spansion, Inc., and Advanced Micro Devices, but many of the performance details are not in the open literature.^{4,10–12} An ongoing effort to commercialize molecular memory is based on redox charge storage in porphyrins and related devices, with the goal of higher charge density, lower cost, and longer retention than conventional DRAM.¹³

Our laboratory has investigated molecular junctions based on TiO₂ which show memory characteristics, including write/erase speeds of 50 μ s–1 ms and retention of tens of minutes.^{14–17} The core concept of these devices is “dynamic doping”, in which

- (1) Kozicki, M. N.; Park, M.; Mitkova, M. *IEEE Trans. Nanotechnol.* **2005**, *4*, 331–338.
- (2) Kozicki, M. N.; Mitkova, M.; Park, M.; Balakrishnan, M.; Gopalan, C. *Superlattices Microstruct.* **2003**, *34*, 459–465. Mitkova, M.; Kozicki, M. N.; Kim, H. C.; Alford, T. L. *Thin Solid Films* **2004**, *449*, 248–253.
- (3) Suppes, G. M.; Deore, B. A.; Freund, M. S. *Langmuir* **2008**, *24*, 1064–1069.
- (4) Krieger, J. H.; Spitzer, S. Switchable memory diode—a new memory device. U.S. Patent 7,157,732, 2007.
- (5) Lai, Q.; Zhu, Z.; Chen, Y.; Patil, S.; Wudl, F. *Appl. Phys. Lett.* **2006**, *88*, 133515–133513.
- (6) Krieger, J. H.; Trubin, S. V.; Vaschenko, S. B.; Yudanov, N. F. *Synth. Met.* **2001**, *122*, 199.

- (7) Sung Hoon, K.; Crisp, T.; Kymissis, I.; Bulovic, V. *Appl. Phys. Lett.* **2004**, *85*, 4666.
- (8) Green, J. E.; Wook Choi, J.; Boukai, A.; Bunimovich, Y.; Johnston-Halperin, E.; Delonno, E.; Luo, Y.; Sheriff, B. A.; Xu, K.; Shik Shin, Y.; Tseng, H.-R.; Stoddart, J. F.; Heath, J. R. *Nature* **2007**, *445*, 414.
- (9) Jang, Y.; Hwang, S.; Kim, Y.; Jang, S.; Goddard, W., III *J. Am. Chem. Soc.* **2004**, *126*, 12636–12645. Melosh, N. A.; Boukai, A.; Diana, F.; Gerardot, B.; Badolato, A.; Petroff, P. M.; Heath, J. R. *Science* **2003**, *300*, 112–115. Luo, Y.; Collier, C. P.; Jeppesen, J. O.; Nielsen, K. A.; Delonno, E.; Ho, G.; Perkins, J.; Tseng, H.-R.; Yamamoto, T.; Stoddart, J. F.; Heath, J. R. *ChemPhysChem* **2002**, *3*, 519–525.
- (10) Mandell, A.; VanBuskirk, M. A.; Spitzer, S.; Krieger, J. H. Polymer memory device with variable period of retention time. U.S. Patent 7,199,394, 2007. Bulovic, V.; Mandell, A.; Perlman, A. Molecular memory device. U.S. Patent 6,781,868, 2004.
- (11) Mandell, A.; Krieger, J. H.; Sokolik, I.; Kingsborough, R. P.; Spitzer, S. Three dimensional polymer memory cell systems. U.S. Patent 7,307,338, 2007.
- (12) Kingsborough, R.; Sokolik, I.; Gaun, D.; Kaza, S.; Pangrle, S.; Nickel, A.; Spitzer, S. Memory elements using organic active layer. U.S. Patent 7,102,156, 2006.

an applied electric field causes injection of electrons into the conduction band of TiO₂, followed by reduction to a metastable Ti^{III} oxide. The conductivity of the Ti^{III} oxide is orders of magnitude higher than that of Ti^{IV} oxide, thus increasing the conductance of the molecular junction by at least a factor of 100. The process is reversible with an “erase” pulse of opposite polarity and is repeatable for at least hundreds of cycles. The Ti^{III} conductive state relaxes back to the nonconducting state in several tens of minutes, while an “erase” pulse restores the low conductance state in <1 ms. The complete junction structure was carbon/molecule/TiO₂/Au, with the molecule being fluorene, nitroazobenzene, or decylamine, and the carbon being a pyrolyzed photoresist film (PPF). The molecular layer acts as a tunneling barrier which permits the applied bias to vary the local Fermi level in the TiO₂ and bring about reduction or oxidation.¹⁴ The roles of Ti and TiO₂ in molecular electronic devices have been reported by other laboratories as well.¹⁸

A drawback of the molecular/TiO₂ devices is the slow “write” and “erase” speeds, presumably due to the structural rearrangements accompanying Ti^{IV} reduction. In addition, the molecular layer is passive, in that it acts only as a tunneling barrier and does not contribute directly to the conductance change responsible for the readout state of the memory device. The current report addresses a significant extension of the concept of “dynamic doping” to include *both* the molecular and TiO₂ layers, by replacing the passive fluorene molecule with a ~20 nm thick layer of polypyrrole (PPy) and then depositing TiO₂ and Au as described previously.¹⁴ PPy is a widely studied conducting polymer which may be p-doped to increase its conductivity from ~10⁻⁹ to 100 S/cm.^{19,20} When the PPy/TiO₂ device is polarized with the PPF positive, as shown in the drawing on the right in Figure 1, an electrochemically driven redox process should oxidize the PPy to produce a conducting state, while the TiO₂ is also reduced to produce electrons in its conduction band. Thus, both polymer and oxide phases are “doped” by the applied bias, and the resulting conductive junction may be returned to its low-conductivity state by a reverse bias pulse. Described herein

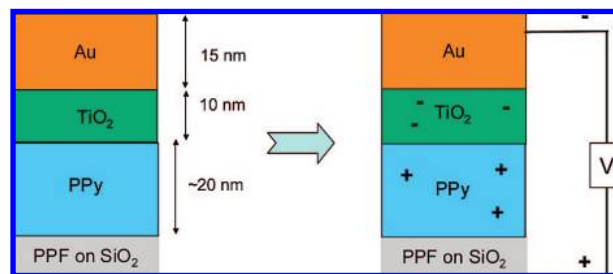


Figure 1. Schematics of junction structure of PPF/PPy/TiO₂/Au. Left, the low-conductance “erased” state; right, the high-conductance “set” state.

are the characteristics of the PPy/TiO₂ junction, including its potential as a low-volatility microelectronic memory element.

Experimental Section

Molecular junctions were of the “crossbar” configuration described in detail previously,^{14,15,21} consisting of the intersection of a 0.5 mm wide strip of PPF and a 0.5 mm strip of TiO₂ and Au. The 0.5 mm strips of PPF ($\rho = 0.006 \Omega\text{-cm}$, roughness <0.5 nm rms) were prepared lithographically on SiO₂ on silicon, as described previously.²² Electrochemical deposition of polypyrrole on PPF was carried out in a 0.1 M solution of pyrrole in acetonitrile solution containing 0.1 M tetrabutylammonium tetrafluoroborate as supporting electrolyte. A constant oxidation current of 50 μA for 200 s, followed by reduction at constant potential (-1 V for 75 s), produced a ~20 nm thick film of nominally undoped PPy. The PPy thickness was determined by variable-angle spectroscopic ellipsometry (Woolam, Inc.) on two separate PPF samples to be 20.0 ± 3.7 and 17.7 ± 4.5 nm. For “control” junctions containing a ~1.7 nm fluorene (FL) layer in place of a conducting polymer, the FL was bonded to the PPF by reduction of fluorene diazonium ion, as described previously.¹⁴

Strips of TiO₂ and gold (0.5 mm wide) were deposited through a shadow mask perpendicular to the PPF strips by electron beam evaporation to yield a junction area of 0.0025 cm². The TiO₂ was deposited from rutile with an electron beam evaporator (Lesker PVD-75) pumped to $<1 \times 10^{-6}$ Torr and then backfilled with O₂ to $\sim 1 \times 10^{-5}$ Torr. After deposition of TiO₂ at a rate of 0.02 nm/s, the O₂ supply was turned off, and then Au was deposited through the same shadow mask at 0.03 nm/s with a backpressure of $<2 \times 10^{-6}$ Torr. The thicknesses of metal and metal oxide were determined by a quartz crystal microbalance in the deposition chamber. The junction designation PPF/PPy(20)/TiO₂(10)/Au(15) indicates a 20 nm thick polypyrrole layer, 10 nm thick TiO₂ layer, and 15 nm thick gold layer, and this configuration was used throughout unless indicated otherwise. Four parallel PPF stripes yielded eight junctions per sample. Some junctions were made without added O₂ during TiO₂ deposition, with minimal effects on device performance. Several samples were made with Pt as the top contact instead of Au, and their performance was quite similar. Pt devices were not studied extensively due to the relatively high temperatures associated with Pt e-beam deposition.

Electronic characteristics of the completed junctions were determined in air using a three-wire arrangement described previously,^{14,15} with the “- sense” and “- drive” connected together on the Au contact of the devices. This arrangement corrects for ohmic error in the PPF, which results from the several hundred ohms resistance of the PPF and probe contacts. Experiments were conducted with a National Instruments 6110 DAQ board, an SRS 570 current amplifier, and Labview software. The transient response time of the board and amplifier was ~1 μs , with a maximum acquisition rate of 5 megasamples/s at 12-bit resolution. In all cases,

- (13) Kuhr, W. G. *Interface (The Electrochemical Society)* **2004**, *13*, 34–38. Roth, K. M.; Yasserli, A. A.; Liu, Z. M.; Dabke, R. B.; Malinovskii, V.; Schweikart, K. H.; Yu, L. H.; Tiznado, H.; Zaera, F.; Lindsey, J. S.; Kuhr, W. G.; Bocian, D. F. *J. Am. Chem. Soc.* **2003**, *125*, 505–517. Roth, K. M.; Yasserli, A. A.; Liu, Z.; Dabke, R. B.; Malinovskii, V.; Schweikart, K. H.; Yu, L.; Tiznado, H.; Zaera, F.; Lindsey, J. S.; Kuhr, W. G.; Bocian, D. F. *J. Am. Chem. Soc.* **2003**, *125*, 505–517. Bocian, D. F.; Kuhr, W. G.; Lindsey, J. S. High density non-volatile memory device. U.S. Patent 6,381,169, 2002.
- (14) Wu, J.; Mobley, K.; McCreery, R. *J. Chem. Phys.* **2007**, *126*, 24704.
- (15) McCreery, R.; Wu, J.; Kalakodimi, R. *J. Phys. Chem. Chem. Phys.* **2006**, *8*, 2572–2590.
- (16) McGovern, W. R.; Anariba, F.; McCreery, R. *J. Electrochem. Soc.* **2005**, *152*, E176–E183.
- (17) Nowak, A.; McCreery, R. *J. Am. Chem. Soc.* **2004**, *126*, 16621–16631.
- (18) Blackstock, J. J.; Stickle, W. F.; Donley, C. L.; Stewart, D. R.; Williams, R. S. *J. Phys. Chem. C* **2007**, *111*, 16–20. Lau, C. N.; Stewart, D. R.; Bockrath, M.; Williams, R. S. *Appl. Phys. A: Mater. Sci. Processing* **2005**, *A80*, 1373–1378. Richter, C. A.; Stewart, D. R.; Ohlberg, D. A. A.; Williams, R. S. *Appl. Phys. A: Mater. Sci. Processing* **2005**, *80*, 1355–1362.
- (19) Vercelli, B.; Zotti, G.; Berlin, A.; Grimoldi, S. *Chem. Mater.* **2006**, *18*, 3754–3763. Epstein, A. J.; Lee, W. P.; Prigodin, V. N. *Synth. Met.* **2001**, *117*, 9–13. Bredas, J. L.; Scott, J. C.; Yakushi, K.; Street, G. B. *Phys. Rev. B* **1984**, *30*, 1023–1025.
- (20) Geetha, S.; Trivedi, D. C. *Mater. Chem. Phys.* **2004**, *88*, 388.
- (21) Anariba, F.; Steach, J.; McCreery, R. *J. Phys. Chem. B* **2005**, *109*, 11163–11172.

- (22) Ranganathan, S.; McCreery, R. L. *Anal. Chem.* **2001**, *73*, 893–900. Ranganathan, S.; McCreery, R. L.; Majji, S. M.; Madou, M. J. *Electrochem. Soc.* **2000**, *147*, 277–282.

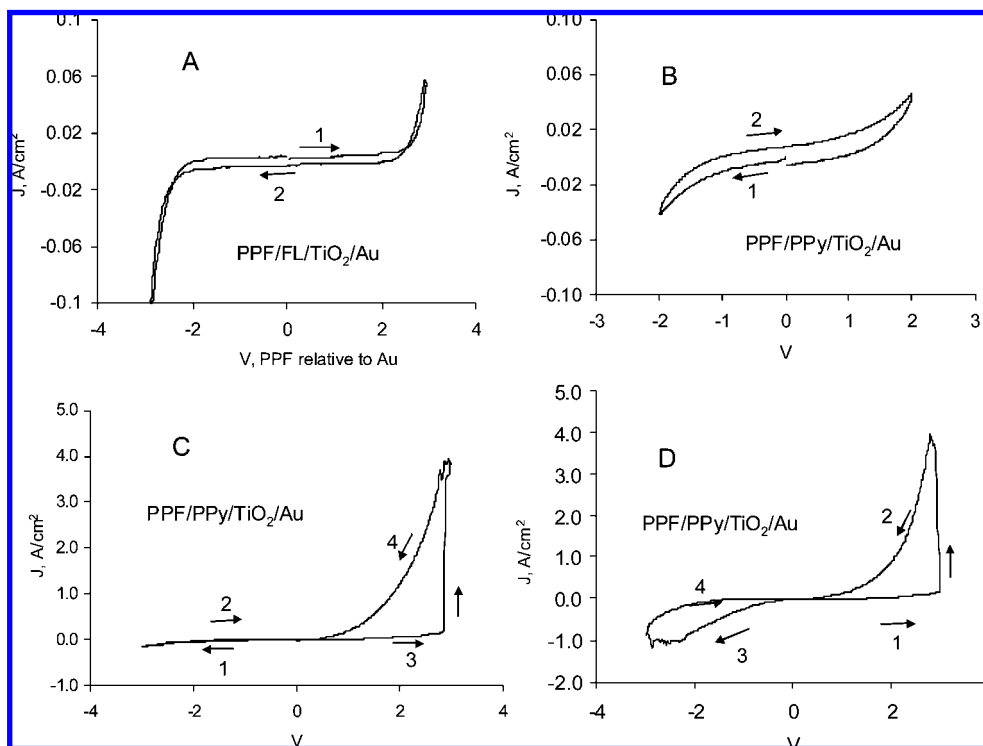


Figure 2. Current density vs voltage (J/V) curves for PPF/FL/TiO₂/Au (A) and PPF/PPy/TiO₂/Au (B–D) junctions at a scan rate of 1000 V/s. Arrows indicate scan direction, in the order indicated, and voltage is stated as PPF relative to Au. Scans A and D were initiated in the positive direction from zero bias, while scans B and C were initiated in the negative direction from zero bias.

the polarity is stated as PPF relative to Au, and the current density is positive for electron flow from Au through the junction to PPF. Electronic experiments consisted of voltage scans and pulses, as described for each figure in the text. Samples were characterized electronically in ambient after removal from the e-beam chamber, and their electronic response did not change significantly for at least 1 week after exposure to air. Contacts to PPF and Au were made with tungsten probes with the aid of three-axis translation stages.

Results and Discussion

Figure 2 shows current density vs voltage curves for linearly scanned voltages on two different device structures, with the numbered arrows indicating the order and direction of the voltage scans. Panel A is from a PPF/FL(1.7)/TiO₂(10)/Au device with a redox-inactive molecular layer, which has been described in detail previously¹⁴ but is included here for reference. The sharp increase in current at ~ 3 V for either polarity is due to injection of electrons into the TiO₂ conduction band. Panel B is the PPF/PPy(20)/TiO₂(10)/Au(15) device response to a voltage scan over the ± 2 V range. The polymer did not dramatically affect the response for this voltage range, although a higher leakage current is observed in this case. In panel C, the voltage was initially scanned to -3 V (PPF relative to Au), and no rapid rise in current was observed. Scans between 0 and -3 V may be repeated at will, with no observable changes in the j - V curves with additional cycles. However, if the voltage is scanned to $+3$ V after the -3 V scan, a sudden increase in current is observed between 2.5 and 3 V, followed by significant hysteresis on the return scan. Panel D shows that if the scan is initiated in the positive direction first, the sudden increase and hysteresis are observed, followed by hysteresis of the opposite sense during the negative scan. The current increase and hysteresis are very consistent across all junctions on a given

sample as well as between different samples: the sudden current increase always occurred when the PPF was biased positive, and the current always decreased to its initial value when the PPF was biased negative, as shown in panel D.

The sudden increase in current shown in Figure 2C,D is reminiscent of the behavior of PPF/molecule/TiO₂ devices in which the top contact was either Cu or Ag.²³ When the Cu or Ag was biased positive beyond a certain threshold, metal filaments formed erratically and suddenly, presumably by oxidation of the metal, transport of the metal ion in the electric field, and then reduction back to the metal at the negatively biased electrode. As was the case in Figure 2D, filament formation showed hysteresis in opposite directions for opposite polarity, and the filaments could be made and destroyed repeatedly. However, metal filaments are unlikely to mediate the conductance change in PPF/PPy/TiO₂/Au devices shown in Figure 2 for several reasons. First, the conductance increase occurs when the PPF is positive, and there is no known process involving oxidation and migration of carbon to form filaments. Second, the sudden increase in current apparent in Figure 2C,D was never observed with PPF/fluorene/TiO₂/Au devices which were studied extensively.^{14,15} Third, filament behavior observed for Ag and Cu devices was not observed for any junctions made with Au as the top contact, either in past or present experiments, for a variety of molecules and metal oxides.^{14,15,17,23,24} As will be discussed later on the basis of additional experimental evidence, it is likely that “filaments” of oxidized conducting polymer are formed in the PPy during a positive bias, and the

(23) Ssenyange, S.; Yan, H.; McCreery, R. L. *Langmuir* **2006**, *22*, 10689–10696.

(24) McCreery, R. L.; Viswanathan, U.; Kalakodimi, R. P.; Nowak, A. M. *Faraday Discuss.* **2006**, *131*, 33–43.

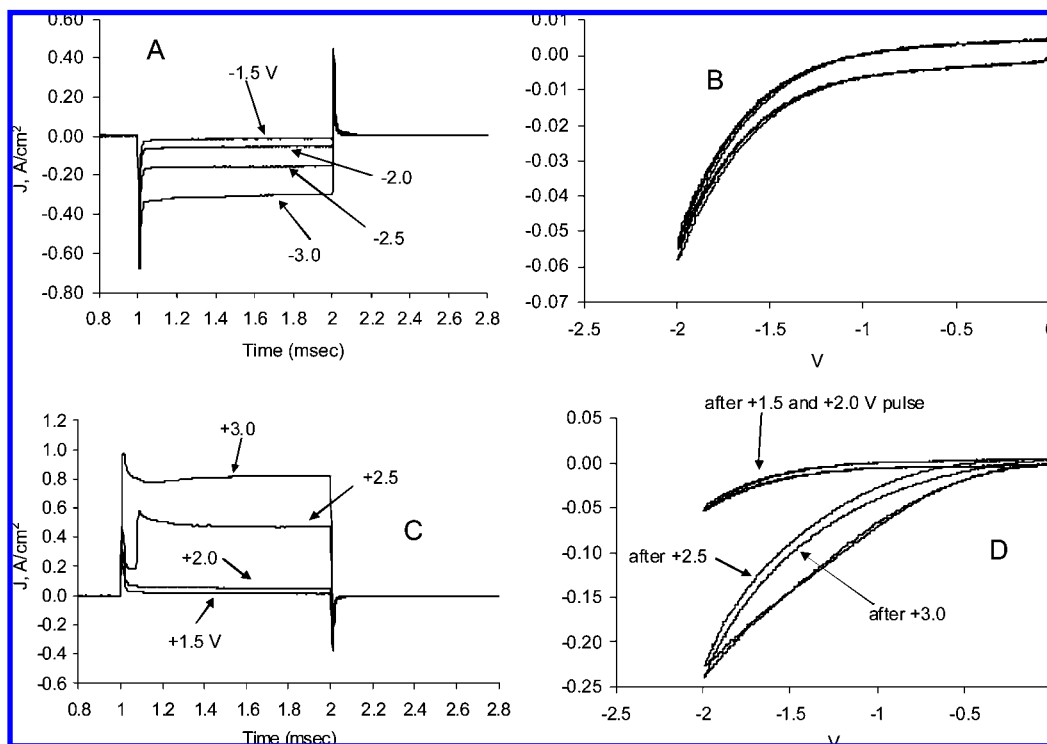


Figure 3. Voltage pulses of increasing magnitude applied to a PPF/PPy(20)/TiO₂(10)/Au junction after 1 ms at zero bias, returning to $V = 0$ at the end of the pulse. (A) Response to 1 ms pulses of amplitude -1.5 to -3.0 V. (B) J/V curves before and after applying the pulses of panel A. (C) Response to 1 ms voltage pulses of amplitude $+1.5$ to $+3.0$ V. (D) J/V curves before and after applying positive pulses. All scans were at 1000 V/s.

much higher conductivity of these “doped” PPy regions is responsible for the sudden conductance change.

The behavior of PPF/PPy/TiO₂/Au junctions in response to voltage pulses of increasing magnitude is shown in Figure 3. For both negative (A,B) and positive (C,D) voltage pulses, current/voltage curves between 0 and -2 V were obtained to assess the effect of the pulse. Figure 3A shows the responses to square, 1 ms pulses with amplitudes increasing negatively from -1.5 to -3.0 V. Following a capacitive spike, the current is essentially constant during the pulse, with the current magnitude corresponding to that expected from the J/V curve of Figure 2D, segment 4. As shown in Figure 3B, these negative pulses have insignificant effects on the J/V curves before and after each pulse, implying that the junction is not perturbed by negative pulses, even for pulses as negative as -4.5 V. The response to positive pulses is quite different, as shown in Figure 3C. For a $+2.5$ V, 1 ms pulse, there is a sudden increase in current early in the pulse, and a subsequent pulse to $+3.0$ V shows a significantly increased current magnitude. The J/V curves in Figure 3D indicate that the $+1.5$ and $+2.0$ V pulses have no effect on the J/V curve, while $+2.5$ and $+3.0$ V pulses show a persistent and significant increase in junction conductance.

After consideration of the J/V curve of Figure 2D, the conductance increase resulting from a positive pulse should be reversed by a negative pulse of sufficient magnitude. Figure 4 illustrates a complete “memory cycle” for six PPF/PPy/TiO₂/Au junctions on the same sample. The initial J/V curves are overlaid in panel A and exhibit a small capacitive current, as expected for the fast scan rate of 1000 V/s. Figure 4B shows J/V curves for the same six junctions after each was subjected to a 100 ms pulse to $+3$ V. The average resistance decreased ($V = \pm 0.2$ V) from 20.6 k Ω to 280 Ω as a result of the positive voltage pulse. Panel C shows the J/V curves after a negative pulse to -3 V, with all six curves superimposed for the six

junctions. Five of the six were “erased” as a consequence of the negative pulse, with the average resistance for all six now being 18.6 k Ω . A complete cycle is shown in Figure 4D, which superimposes the J/V curves obtained on the initial junction and after the $+3$ V “write” pulse and the -3 V “erase” pulse. The observed junction resistance and associated statistics for 28 PPy/TiO₂ junctions on four samples made at different times are shown in Table 1, with Figure 4 derived from data on sample 3. The standard deviations of the resistance values within and between samples are fairly large, ranging from 20 to 60%; however, they are much smaller than the change in resistance when the device is “set” (a factor of 20–150). Therefore, even with relatively high variation in junction resistance, the distinction between the “set” and “initial” conductance states can be made clearly, with statistical validity. As will be noted below, junctions occasionally failed to erase completely, as apparent in Figure 4C.

The dynamics of the PPy/TiO₂ are shown in Figure 5 for “set” and “erase” pulses of $+3$ and -3 V, respectively. As shown in panel A, the “write” pulse duration may be decreased from 100 ms to 10 μ s, which was as fast as the equipment used could acquire data. While there is some decrease in the magnitude of the current with decreasing pulse duration, the “set” state is only weakly dependent on write time. This observation is consistent with the sudden increase in current observed in panels C and D, implying that the “write” process is quite fast but also self-limiting. Figure 5B shows a series of J/V curves obtained at various times after a 50 μ s, $+3$ V “write” pulse, with the device at open circuit between the various scans. After an initial decrease in the current of the “set” state within 30 min after the write pulse, further decreases in current are quite slow, amounting to $\sim 60\%$ in 7 days. However, the “off” state is restored immediately after 7 days with a -3 V “erase” pulse.

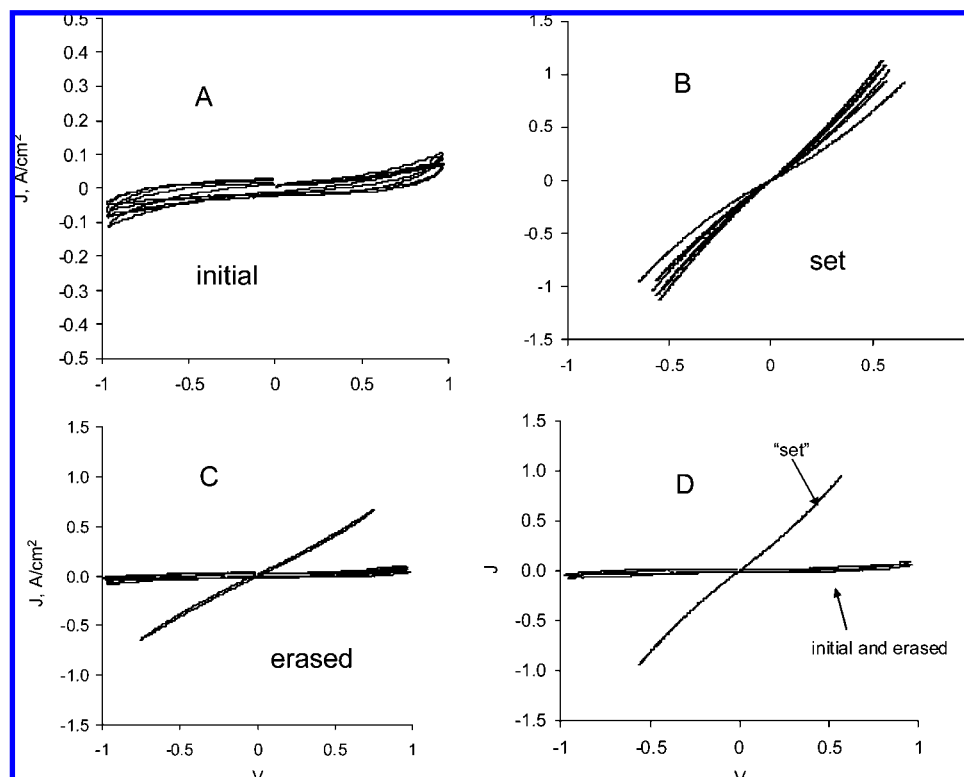


Figure 4. Current density/voltage (J/V) curves (1000 V/s) for six different PF/PPy(20)/TiO₂(10)/Au junctions before and after applying 100 ms “set and “erase” pulses of +3 and −3 V, respectively: (A) initial J/V curves; (B) after “set” pulse; (C) after “erase” pulse. Panel D is an overlay of J/V curves before and after “set” and “erase” pulses.

Table 1. Junction Resistance (in Ω) at Low Voltage (± 0.2 V) for Four PPF/PPy/TiO₂/Au Samples

junction no.	sample 1		sample 2		sample 3		sample 4	
	initial resistance	initial resistance	initial resistance	set resistance	off/on ^b	initial resistance	set resistance	off/on ^b
1	43180	9232	40652	280	145.2	41684	292	142.8
2	29926	14540	12640	240	52.7	50804	852	59.6
3	21425	19248	18160	228	79.6	29940	1480	20.2
4	31325	43324	9800	380	25.8	35668	1520	23.5
5	23114	15668	24752	292	84.8	48240	1160	41.6
6	7366	4620	18120	252	71.9	41860	1228	34.1
7	32196	15536				77700	288	
8		37712						
mean	26933	19985	20687	279	77	46557	974	54
rsd ^a	0.414	0.676	0.535	0.198	0.520	0.332	0.531	0.856

^a Relative standard deviation. ^b “off/on” is the ratio of the “erased” resistance to the “set” resistance.

The magnitude of the voltage required to “set” and “erase” the polymer junctions depended on the thickness of the polypyrrole film. Figure 6A shows a memory cycle for a PPy/TiO₂ junction with a ~ 20 nm PPy film and 1 ms voltage pulses 3.5 V in magnitude, with behavior similar to that shown in Figures 3 and 4. If the deposition time for PPy was increased to 1000 s, with all other parameters identical, a much thicker film of PPy is expected, in the range of 80–100 nm. A memory cycle for the thicker PPy case is shown in Figure 6B, again for 3.5 V pulses. The “set” and “erase” pulses have no effect for either 1 or 100 ms duration on the thicker film. As shown in Figure 6C, conductance switching is restored in the thicker junction if the pulse magnitude is increased to 6.7 V. Although thinner films of PPy resulted in junctions that switched at lower voltage, the yield and reproducibility were low.

The behavior of PPF/PPy/TiO₂/Au junctions shown in Figures 2 and 5 is entirely consistent with the “dynamic doping”

mechanism proposed for PPF/fluorene/TiO₂/Au devices,¹⁴ but with a change in the active switching element. The fluorene/TiO₂ junctions became more conductive when the Au electrode was biased negative, with the fluorene acting as a tunneling barrier. Switching in TiO₂ is very sensitive to the presence of water, due to the dependence of the reduction of Ti^{IV} to Ti^{III} oxide on the presence of hydrated Ti^{IV} sites.²⁵ As shown in Figure S1 in the Supporting Information, the “set” process in PPF/fluorene/TiO₂/Au junctions is completely suppressed if the device is stored in a drybox for >24 h. The conductance switching observed in PPy/TiO₂ devices is not only much faster and longer lived than that in fluorene/TiO₂, but it is insensitive to humidity. As shown in Figure 7, the memory effect actually improves in the dry atmosphere for PPy/TiO₂ devices, with the

(25) Szczepankiewicz, S. H.; Colussi, A. J.; Hoffmann, M. R. *J. Phys. Chem. B* **2000**, *104*, 9842–9850.

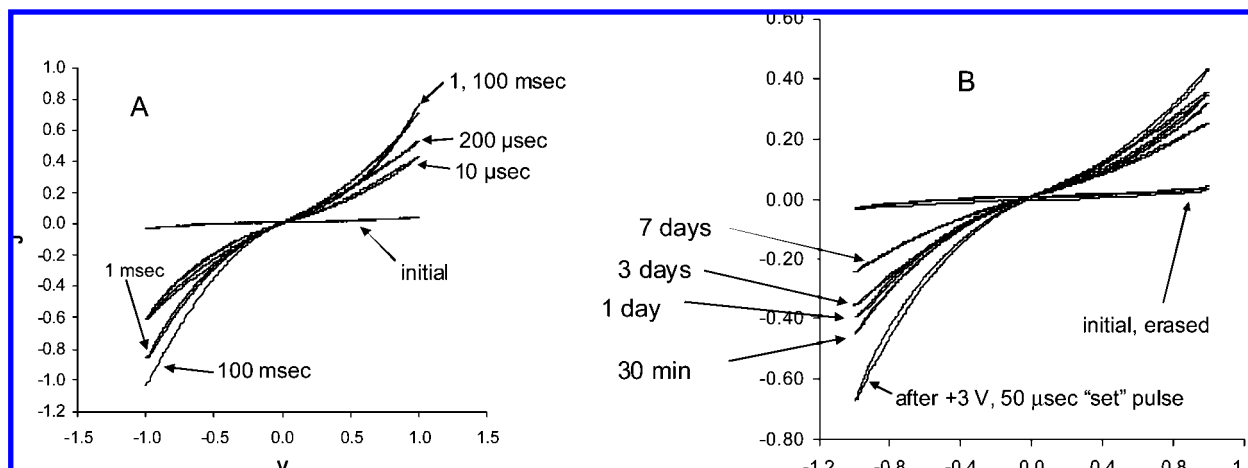


Figure 5. (A) Effect of duration of “set” pulse for a PPF/PPy/TiO₂/Au junction. “Initial” is the *J/V* curve before the set pulse, and the labeled curves are after +3 V set pulses of the indicated lengths. Junction was erased between successive pulses and always started with the response indicated as “initial”. (B) Repeated *J/V* scans obtained at the indicated times after a 50 μs, +3 V pulse, with junction at open circuit between scans. Scans 1000 V/s in all cases.

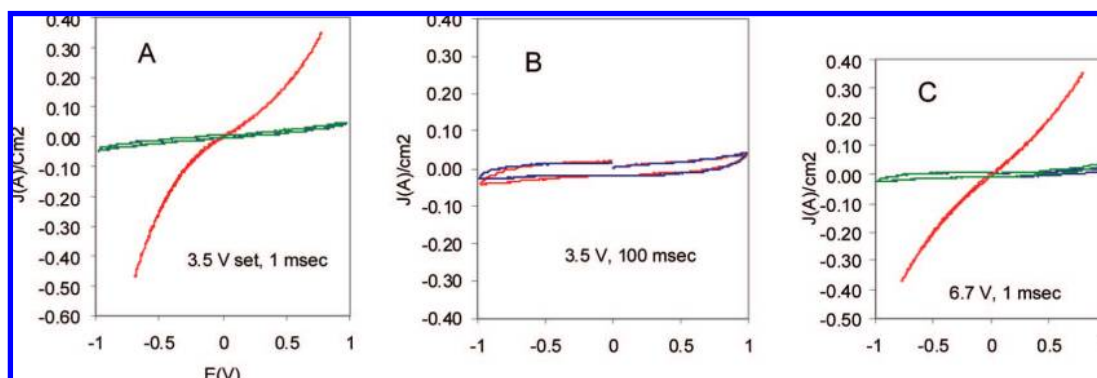


Figure 6. Memory response for PPF/PPy/TiO₂/Au junctions having different PPy thickness. (A) The “standard” junction made with 200 s of pyrrole oxidation at 50 μA, for a 1 ms, +3.5 V “set” pulse. (B) A junction made and tested identically but made with 1000 s of pyrrole oxidation. (C) Same device as in panel B, but with a 1 ms, +6.7 V “set” pulse.

“set” current increasing over that observed in air. The observations support the hypothesis that the polypyrrole rather than the TiO₂ is the primary switching element in the device, with positive bias causing oxidation of the PPy to form conducting polarons. The PPy “doping” is likely accompanied by some electron injection into the TiO₂, but the major conductance change is in the polymer. The fluorene/TiO₂ devices may be considered “control” junctions which contain TiO₂ but lack a conducting polymer. Compared to fluorene/TiO₂, the PPy/TiO₂ devices have much longer retention (~1 week vs ~30 min), faster switching (10 μs vs ~1 ms), and less sensitivity to humidity. Once the polymer is switched to its conducting state, the current is presumably limited by the TiO₂ conductance, resulting in the nearly linear *J/V* behavior apparent in Figure 4B. The TiO₂ conductance is determined by small amounts of Ti^{III} or Ti^{II} oxides, either present initially or formed during the “write” pulse.^{14,16}

As shown in Figure 8, conductance switching is also readily observed with electrochemically deposited polythiophene as well as spin-coated poly(3-hexylthiophene) instead of polypyrrole. The conductance changes are qualitatively similar to those observed with PPy, although they were not studied in the same detail. When TiO₂ was replaced with SiO₂ to make PPF/polythiophene/SiO₂/Au devices, the conductance was much lower, and switching was not observed. The band gap in SiO₂ is much larger than that in TiO₂ (~9 eV vs ~3 eV), making a

barrier too high for significant current flow. It is possible that the polymer is still oxidized in SiO₂ devices, but the much larger resistance of the silica layer prevents observation of an associated conductance change. Although the TiO₂ does not appear to significantly change conductance in PPy/TiO₂ junctions, it may act as an electron acceptor, which permits oxidation of the polypyrrole. As reported previously,¹⁴ it is possible to inject electrons into TiO₂ to generate a space charge, and these electrons may be trapped or may even cause reduction of Ti^{IV} to Ti^{III}. The observation that PPy/TiO₂ devices produce larger and more stable conductance changes than fluorene/TiO₂ junctions indicates that the polymer is the primary “switch” in PPy/TiO₂ devices, but it is likely that both polymer and oxide undergo redox reactions, as indicated in Figure 1.

The much longer retention of PPy/TiO₂ junctions (~7 days) compared to fluorene/TiO₂ analogues (~30 min) was unexpected. Although the availability of two redox systems in PPy/TiO₂ should stabilize the charge more efficiently than the one redox system present in fluorene/TiO₂, the conducting state should still have a significant space charge resulting from the “set” pulse, which should promote discharge of the device back to the low-conductance state. Furthermore, a significant space charge would be expected to generate a barrier to conduction, as proposed for the origin of rectification in NAB/TiO₂

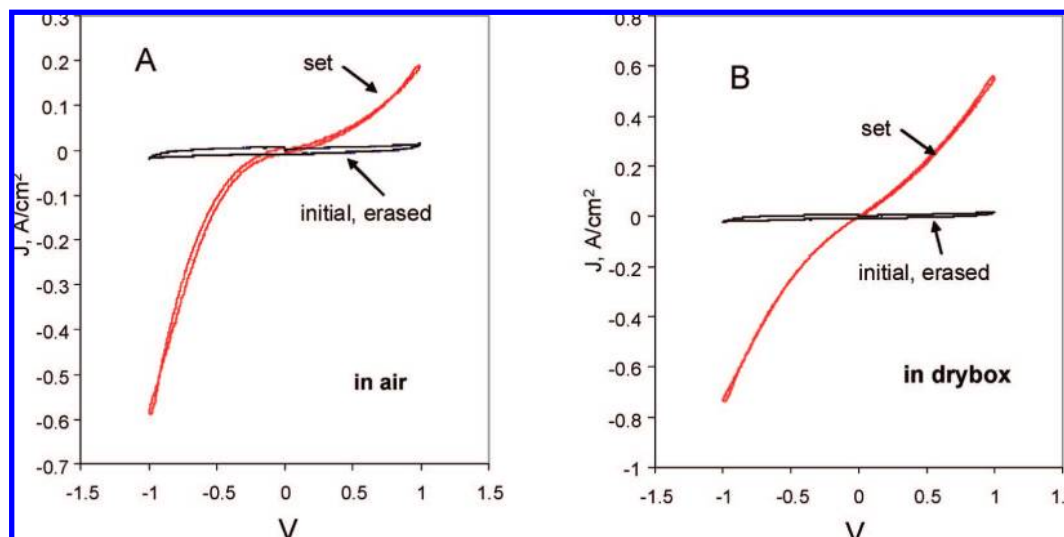


Figure 7. Effect of oxygen and humidity on a PPF/PPy(20)/TiO₂(10)/Au junction. (A) Acquired in air for +3 V, 50 μs “set” and -3 V, 1 ms “erase” pulses. (B) Acquired using the same conditions on the same junction, after storage in a drybox for ~24 h. Figure S1 in the Supporting Information shows that a dry atmosphere completely suppresses the memory response for PPF/fluorene/TiO₂/Au junctions.

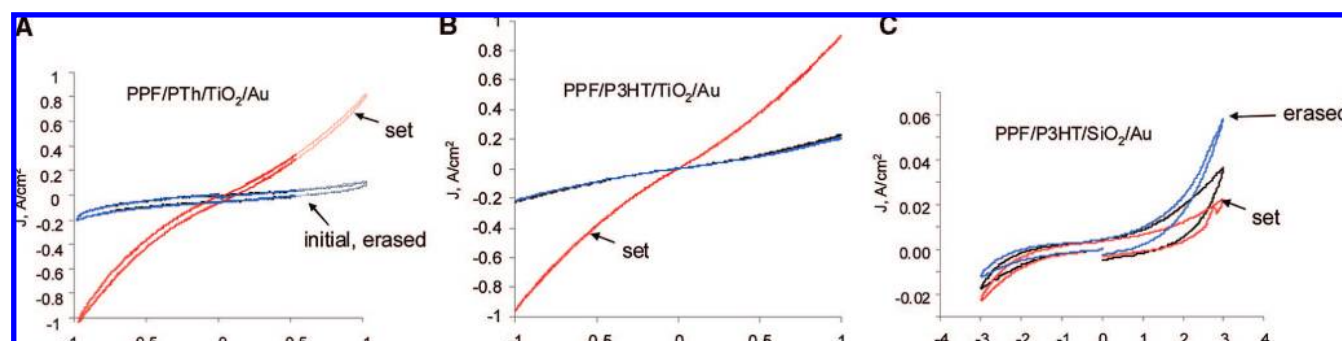


Figure 8. Memory cycles for PPF/polymer/metal oxide/Au junctions with varying composition. In all cases, 1000 V/s scans were obtained before and after 100 ms “set” and “erase” pulses to ±3 V (A,B) or ±5 V (C). (A) PPF/polythiophene/TiO₂/Au, with polythiophene (PTh) grown electrochemically from thiophene in acetonitrile. (B) Same as in panel A, but polymer was spin-coated poly(3-hexylthiophene) (P3HT). (C) Same as in panel B, but with SiO₂ substituted for TiO₂.

junctions.^{17,26} However, the magnitude of the charge responsible for generating the conducting state in the polymer may be quite small, since low doping levels are required to significantly increase the polypyrrole conductivity. Undoped PPy has a reported conductivity of $\sim 10^{-9}$ S/cm, with a maximum conductivity in the doped state of ~ 200 S/cm.²⁰ Various reports indicate that oxidation of a few percent of the pyrrole rings in PPy greatly increases conductivity, with a maximum reached at ~ 0.15 hole/pyrrole ring.²⁷ However, lightly doped PPy with a conductivity of 10^{-4} S/cm would exhibit a resistance of only 8Ω in a 0.0025 cm^2 junction with a PPy thickness of 20 nm. Therefore, the changes in conductance that occur in PPy/TiO₂ devices during a “set” pulse are possible with very light doping, much less than 0.01 hole/pyrrole unit. An additional factor causing long retention may be the availability of mobile ions to compensate the charge associated with PPy oxidation. Since the doping level might be quite low, residual ions from water

or the electrolyte used for PPy formation may be sufficient to balance the cationic polarons formed during the “set” pulse. If mobile ions are present, the PPy/TiO₂ device contains all of the elements of a conventional redox cell: two redox systems, an electrolyte, and two electrodes. Although ion transport would be expected to be slow in a solid-state device, the distances ions need move are very short, a few tens of nanometers at most. We emphasize that there is no direct evidence for the involvement of mobile ions in PPy/TiO₂ devices, but their presence and possible importance are difficult to rule out. Experiments involving intentional addition of mobile ions to the polymer layer are currently in progress.

PPF/PPy/TiO₂/Au junctions were tested for endurance by repeated read/set/read/erase cycles similar to those shown in Figure 4. The “set” pulse was 100 ms at 3 V, and the “erase” was -3 V, 1000 ms, both chosen to represent parameters at the extremes of the pulse durations studied. The junction state was “read” by 1 ms, -1 V pulses after each “set” and “erase”, and voltammetric scans were acquired after blocks of ~ 500 set/erase cycles. Figure 9A shows the first memory cycle for a PPF/PPy/TiO₂/Au device, with the “initial” and “erased” curves being indistinguishable. Figure 9B shows *J/V* curves obtained after the “set” and “erase” pulses of the first, 535th, 1060th, and 1600th set/erase cycles on the same device. The *J/V* curves of

(26) Kalakodimi, R. P.; Nowak, A.; McCreery, R. L. *Chem. Mater.* **2005**, *17*, 4939–4948.

(27) Chakrabarti, S.; Das, B.; Banerji, P.; Banerjee, D.; Bhattacharya, R. *Phys. Rev. B* **1999**, *60*, 7691–7694. Chance, R. R.; Brédas, J. L.; Silbey, R. *Phys. Rev. B* **1984**, *29*, 4491. Feldman, B. J.; Burgmayer, P.; Murray, R. W. *J. Am. Chem. Soc.* **1985**, *107*, 872–878. Zotti, G.; Zecchin, S.; Schiavon, G.; Vercelli, B.; Berlin, A.; Dalcanale, E.; Groenendaal, L. B. *Chem. Mater.* **2003**, *15*, 4642–4650.

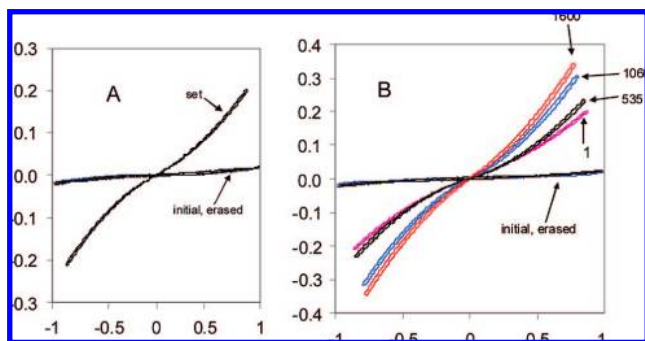


Figure 9. (A) Initial memory cycle for 3 V, 100 ms “set” and “erase” pulses for a PPF/PPy/TiO₂/Au junction. (B) Initial and “set” *J/V* curves for the 0th, 535th, 1060th, and 1600th memory cycles, as indicated. All initial and erased curves were superimposable. Scan rate was 1000 V/s in all cases.

the “erased” junction are all virtually identical, while the “set” current increases gradually with the number of cycles. The junction resistance monitored at -1 V for each cycle switched between 1.8 ± 0.8 and 17.7 ± 3.8 k Ω for the “set” and “erased” states, respectively, and the complete record is shown in Figure S2 of the Supporting Information. Both the “set” and “erased” resistances decreased slowly with repeated cycling, but the ratio of “erased” to “set” resistances measured at -1 V did not show a trend, remaining at 11 ± 4 for a total of 1760 cycles. In $\sim 10\%$ of the switching cycles, the “erase” or “set” process was incomplete, leading to errors in the memory readout. If 8 k Ω is chosen as the threshold for determining if the device is “set” or “erased”, the error rate is $\sim 3\%$. It is likely that this error rate is partly due to difficulty in making good contact with PPF over a long period of time, and more reliable contacts to the external circuit are currently under development.

The substitution of a ~ 20 nm layer of conducting polymer for a redox-inactive molecule in our previously reported PPF/molecule/TiO₂/Au devices significantly enhances their performance as memory devices, as well as increasing the potential for commercial applications in microelectronics. The primary source of enhanced performance is the fast and persistent conductance change permitted by bias-induced redox doping of polypyrrole, rather than the relatively slow changes in TiO₂ conductance that occur in the absence of the polymer. The PPy/TiO₂ junctions can be set and erased at least 2 orders of magnitude faster than fluorene/TiO₂, and they retain the “set” state at least 3 orders of magnitude longer. Readout based on conductance rather than charge storage may permit higher density memory,^{4,8,11,28,29} since the conductance is not subject to leakage of charge which currently limits DRAM density. The cycle life and retention of the PPy/TiO₂ devices are not currently competitive with commercial nonvolatile memory based on “flash” or magnetic devices, but refinement and packaging are likely to result in endurance and retention much longer than the thousands of cycles and >1 week reported here.

There are numerous examples of electronic devices based on conducting polymers,^{30,31} in addition to a rich literature on organic electronic devices.^{7,32} The vast majority of these devices involve layers of polymers or small molecules that are >100

nm thick, and the dominant electron transport mode is “hopping”, involving traps and/or redox exchange. In some cases, polymer devices include intentional electrolyte which is involved in both ion and electron transport in devices such as polymer based p–n junctions^{31,33} and electrochemical diodes and transistors.^{34,35} Unidirectional redox exchange in conducting polymers exposed to electrolyte resulted in diode behavior,³⁴ while electrochemical doping of polypyrrole and polythiophene in electrolyte solution caused large increases in polymer conductivity.³⁵ As noted earlier, memory devices based on conducting polymers have been reported in the open and patent literature, with mechanisms based on the motion of ionic dopants,^{3,4,6,7,10} redox reactions accompanying ion motion,^{4,5} and composites of conducting polymers and electrolyte.^{3,36} The PPF/PPy/TiO₂/Au junctions reported here have several important properties that distinguish them from previous organic and polymer-based electronic devices. First, the polymer and TiO₂ layers are 10–20 nm thick, thus permitting high electric fields and Fermi level shifts which cause redox reactions. Presumably, oxidation of the polypyrrole occurs when an electron can tunnel from the polypyrrole HOMO to the PPF electrode once the HOMO energy has been shifted close to the Fermi level of the PPF in the applied field. Such a shift would require much higher bias in a thick-film device and would likely be impractical. Second, the thin polymer layer permits efficient transport of electrons and possibly ions due to the short distances involved. If a polaron in the oxidized PPy is ~ 5 nm in extent, then only a few “hops” are required to traverse the polymer layer. Using the terminology common to the conducting polymer literature, the very short distance requires a low percolation threshold compared to a more conventional polymer film of >100 nm thickness. The requirement for minimal hopping and its associated low mobility permits the device to support quite large current densities, up to 100 A/cm² in devices examined to date, and the low mobilities common to most organic semiconductors are not manifested in very thin films. Furthermore, the fact that the PPF substrate is ~ 80 times thicker than the polymer layer

- (30) Whiting, G. L.; Snaith, H. J.; Khodabakhsh, S.; Andreasen, J. W.; Breiby, D. W.; Nielsen, M. M.; Greenham, N. C.; Friend, R. H.; Huck, W. T. S. *Nano Lett.* **2006**, *6*, 573–578. Cheng, C. H. W.; Lonergan, M. C. *J. Am. Chem. Soc.* **2004**, *126*, 10536–10537. Burgi, L.; Friend, R. H.; Sirringhaus, H. *Appl. Phys. Lett.* **2003**, *82*, 1482–1484. Milner, R. G.; Arias, A. C.; Stevenson, R.; MacKenzie, J. D.; Richards, D.; Friend, R. H.; Kang, D.-J.; Blamire, M. *Mater. Sci. Technol.* **2002**, *18*, 759–762. deMello, J. C.; Tessler, N.; Graham, S. C.; Friend, R. H. *Phys. Rev. B* **1998**, *57*, 12951.
- (31) Cheng, C. H.; Lin, F.; Lonergan, M. C. *J. Phys. Chem. B* **2005**, *109*, 10168–10178.
- (32) Panzer, M. J.; Frisbie, C. D. *J. Am. Chem. Soc.* **2007**, *129*, 6599–6607. Fritz, S. E.; Mohapatra, S.; Holmes, B. T.; Anderson, A. M.; Prendergast, C. F.; Frisbie, C. D.; Ward, M. D.; Toney, M. F. *Chem. Mater.* **2007**, *19*, 1355–1361. Panzer, M. J.; Frisbie, C. D. *J. Am. Chem. Soc.* **2005**, *127*, 6960–6961. Newman, C.; Frisbie, D.; da Silva Filho, D.; Ewbank, P.; Mann, K. *Chem. Mater.* **2004**, *16*, 4436–4451. Heimel, G.; Romaner, L.; Zojer, E.; Bredas, J. L. *Nano Lett.* **2007**, *7*, 932–940. Tran, E.; Duati, M.; Mullen, K.; Zharnikov, M.; Whitesides, G. M.; Rampi, M. *Adv. Mater.* **2006**, *18*, 1323. Di, C. A.; Yu, G.; Liu, Y.; Xu, X.; Wei, D.; Song, Y.; Sun, Y.; Wang, Y.; Zhu, D.; Liu, J.; Liu, X.; Wu, D. *J. Am. Chem. Soc.* **2006**, *128*, 16418–16419. Facchetti, A.; Yoon, M.-H.; Marks, T. J. *Adv. Mater.* **2005**, *17*, 1705–1725.
- (33) Cheng, C. H. W.; Boettcher, S. W.; Johnston, D. H.; Lonergan, M. C. *J. Am. Chem. Soc.* **2004**, *126*, 8666–8667.
- (34) Thackeray, J. W.; White, H. S.; Wrighton, M. S. *J. Phys. Chem.* **1985**, *89*, 5133–5140. Kittlesen, G. P.; White, H. S.; Wrighton, M. S. *J. Am. Chem. Soc.* **1985**, *107*, 7373–7380.
- (35) Ofer, D.; Crooks, R. M.; Wrighton, M. S. *J. Am. Chem. Soc.* **1990**, *112*, 7869–7879.
- (36) Smits, J. H. A.; Meskers, S. C. J.; Janssen, R. A. J.; Marsman, A. W.; de Leeuw, D. M. *Adv. Mater.* **2005**, *17*, 1169–1173.

(28) Waser, R.; Aono, M. *Nat. Mater.* **2007**, *6*, 833–840.

(29) Scott, J. C.; Bozano, L. D. *Adv. Mater.* **2007**, *19*, 1452–1463. Kozicki, M.; Balakrishnan, M. Programmable metallization cell structures including an oxide electrolyte, devices including the structure and method of forming same. U.S. Patent 7,372,065, 2008.

permits efficient heat conduction away from the polymer. Third, the radical-based polymerization of pyrrole on the graphitic PPF surface during polypyrrole formation may result in covalent bonds between the carbon surface and the polymer. The resulting strong electronic coupling between PPF and polymer is supported by independent spectroscopic evidence³⁷ and should promote electron transfer from the polypyrrole to the PPF under positive bias, resulting in efficient oxidative doping of the polymer layer. Finally, many of the existing devices contain Al, Cu, or Ag as contacts or electrolytes, and these materials are prone to forming conducting filaments which can be “switched” on and off to act as a mechanism for nonvolatile memory.^{23,28} Intentional metal filament formation in the absence of conducting polymers is the basis of several patented memory devices^{1,38} and is always a possibility when the junction contains Cu, Ag, or Al.

Conclusions

Replacement of the redox-inactive fluorene molecule in PPF/fluorene/TiO₂/Au molecular junctions with a ~20 nm film of polypyrrole extends the concept of “dynamic doping” by a redox reaction to a case where both the molecular and oxide layers are redox active. For both polypyrrole and polythiophene molecular layers, the speed and retention of the PPF/polymer/TiO₂/Au devices are far superior to those of PPF/fluorene/TiO₂/Au equivalents, with a polypyrrole junction switching in <10 μs and retaining its “set” state for more than 1 week. Although redox activity of the TiO₂ may be involved in conductance switching, the dominant mechanism for the ob-

served conductance changes is partial oxidation of the polymer film, which generates conducting polarons. The large conductance changes are enabled by the thin molecular and oxide layers in the polymer/TiO₂ devices, which enable sufficient Fermi level shifts under a bias to effect polymer oxidation and associated doping. The superior performance of conducting polymer devices compared to those based on doping of TiO₂ is presumably due to the light doping level required and the relatively rapid redox process in an organic polymer compared to that in a disordered metal oxide.

Acknowledgment. This work was supported by NSERC, the National Research Council, the Alberta Ingenuity Fund, and ZettaCore, Inc. The National Institute for Nanotechnology is operated as a partnership between the NRC and the University of Alberta and is jointly funded by the Government of Canada, the Government of Alberta, and the University of Alberta.

Supporting Information Available: Effects of humidity on fluorene/TiO₂ “control” junctions and an endurance experiment involving 1760 write/read/erase/read cycles. This information is available free of charge via the Internet at <http://pubs.acs.org>.

JA802673W

(37) Tian, H.; Bergren, A. J.; McCreery, R. L. *Appl. Spectrosc.* **2007**, *61*, 1246–1253.

(38) Kozicki, M. Programmable microelectronic devices and method of forming and programming same. U.S. Patent 6,487,106, 2002. Mitkova, M.; Kozicki, M. N.; Kim, H. C.; Alford, T. L. *J. Non-Cryst. Solids* **2004**, *338–340*, 552–556. Gilbert, N. E.; Gopalan, C.; Kozicki, M. N. *Solid-State Electron.* **2005**, *49*, 1813–1819.